# A model for energetic ion generation in an anode plasma

R. E. Duvall, A. Fruchtman, Y. Maron, and L. Perelmutter
*Department of Physics, Weizmann Institute of Science, Rehovot 76100, Israel*

(Received 7 December 1992; accepted 2 June 1993)

Mechanisms for energetic ion generation that could explain the observed ion energies in the anode plasma of a magnetically insulated ion diode [Phys. Rev. A **39**, 5842 (1989)], are discussed. It is suggested that strong electric fields that result from large density gradients on few tens of micrometers near the anode cause the ion acceleration. Steady state as well as time-dependent accelerations are examined.

## I. INTRODUCTION

The ion temperature of a magnetically insulated diode (MID) plasma has a major effect on the device performance, particularly regarding beam divergence. Anode plasmas with ion temperature of about 20 eV have been observed in the MID experiments at the Weizmann Institute.[1-3] This ion temperature is roughly uniform over the plasma, implying that the ions do not acquire their energies in the bulk plasma. In this paper we explore the possibility that ions in MID plasmas are heated in a narrow layer (thickness smaller than 50 $\mu$m) near the anode surface, much narrower than the 1 mm plasma width. It has long been known that the free expansion of a plasma can result in the generation of energetic ions. Ion acceleration due to plasma expansion is known to occur, for example, in vacuum arcs[4-8] and in laser-produced plasmas.[9-14] We suggest that a narrow dense plasma located near the anode of the MID and having high electron temperature expands within this narrow region, resulting in energy transfer from electrons to ions. The plasma flowing out of this region thus contains energetic ions as observed in experiments. We examine this mechanism for both steady-state and time-dependent expansions, and in both planar and spherical geometries.

The dense plasma in our model arises from the rapid ionization of desorbed neutrals. Initially there is a high-density cloud of neutral atoms, having spatial extent of only few tens of micrometers, much smaller than the plasma width of 1 mm. Such neutral clouds are believed to appear on the anode surface in MID's. We assume that by some mechanism the electrons near the anode surface have a higher temperature ($\sim$30–50 eV) than in the bulk of the plasma, even though so far there is no experimental support to this assumption. After electron impact ionization of the neutrals, the resulting plasma expands. The plasma is immersed in a strong magnetic field. However, both ions and electrons are considered unmagnetized; the ions because their Larmor radius is larger than the thickness of the neutral layer, and the electrons because they are collisional. The plasma expansion is therefore ambipolar. The electrons have much higher thermal velocity than the ions, and therefore leave the neutral cloud much faster. As a result of the rapid electron flow from the neutral cloud, a charge imbalance, and therefore an electric field, is produced. The resulting potential hump continues to grow until the electron and ion fluxes are balanced. Ions then gain energy as they fall down the potential hill, while electrons lose energy as they climb out of a potential well. Thus, through this energy exchange, ion acceleration and electron cooling take place. We suggest that this is the mechanism by which ions acquire their kinetic energy.

The flow of neutrals, the plasma production through ionization, the plasma expansion, and the ion acceleration, all these processes occur simultaneously. In some cases certain processes are dominant and the picture is simpler. For simplicity we examine two such cases. In one case a steady state is established, in which the plasma production in the layer is balanced by the flow of plasma from the layer. On a time longer than the transit time, the change in density of the neutrals also changes the steady state. The first case we describe is therefore plasma expansion with ionization in a steady state. The second case we study is a time-dependent expansion. Such an expansion occurs when the supply of neutrals from the anode ceases. If the ionization rate is faster than the rate of plasma expansion, full ionization takes place, followed by a time-dependent expansion of the fully ionized dense plasma. The second case we describe is therefore a time-dependent plasma expansion without accompanying ionization. As we shall show the essential features of the energy transfer from electrons to ions are basically the same for the steady-state and time-dependent expansions.

In addition to the spatial extent and the neutral density, the geometry of the neutral cloud will affect the nature of ion heating. In this paper we consider neutral clouds having either planar or spherical symmetry in space. For a slab of neutrals having no density dependence in the $y$ and $z$ directions, all ion motion is in the $x$ direction, perpendicular to the anode. However, MID measurements indicate that the ion velocity distribution is isotropic. A spherically symmetric ball of neutrals will result in ion motion in every direction. We therefore consider the ion velocity distribution which results from many "half-balls" on the anode surface. Here the anode at $x=0$ divides each ball in half. We are then interested in the ion flow due to all neutrals having $x>0$. Such a distribution of neutrals results in a more isotropic ion velocity distribution than that of a neutral slab. The magnitude of the energy transfer from electrons to ions, however, is not strongly affected by geometry.

In Sec. II we describe the experimental data. In Sec.

 0899-8221/93/5(9)/3399/9/$6.00 © 1993 American Institute of Physics 

Downloaded 04 Feb 2004 to 132.77.4.129. Redistribution subject to AIP license or copyright, see http://pop.aip.org/pop/copyright.jsp

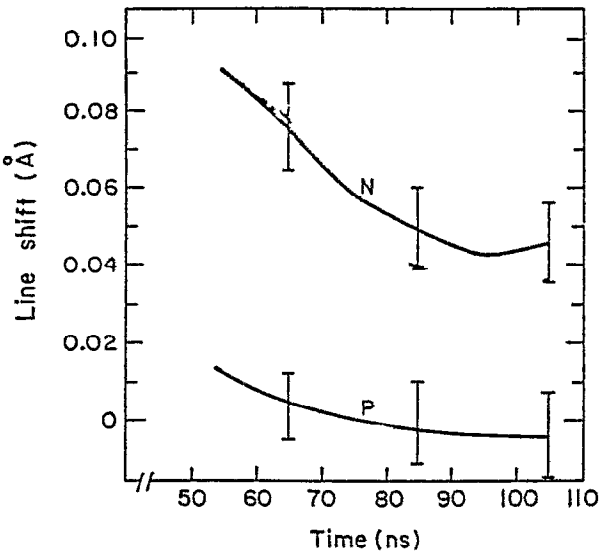


FIG. 1. The blue shift of the CIII 2297 Å line measured at 53° with the normal to the anode ($N$) and the shift measured parallel to the anode ($P$). Each point on the $N$ and $P$ curves is an average of 13 and 12 discharges, respectively.

III we introduce the model used in this paper, independent of geometry. Ions are cold and collisionless, while electrons are collisional and are taken to obey the adiabatic relation $P_e \propto n_e^{\gamma}$, where $P_e$ and $n_e$ are the electron pressure and density, respectively. The electron mass is ignored, and quasineutrality is assumed for the proton electron plasma.

In Sec. IV we solve for the steady-state and time-dependent expansions in planar geometry. The steady-state solution is determined by the parameter $\alpha$, which is the product of the ionization frequency and the ion transit time. In planar geometry, the condition $\alpha < 0.404$ is required for a steady-state flow. For the steady-state flow we found that the initially cold ions can gain energy up to 0.77 of the maximal electron temperature in the layer. For time-dependent expansion, a final ion energy of two to three times the final electron energy results from plasma volume expansion by a factor of 5–8.

In Sec. V we solve for the steady-state and time-dependent expansions in spherical geometry. For spherical geometry we found that the upper limit on $\alpha$ for steady-state flow is about $\alpha = 1.76$, roughly a factor of 4 larger than for planar geometry. In steady state the ions can gain energy up to about 0.7 of the maximal electron temperature in the layer. For time-dependent expansion, a final ion energy of two to three times the final electron energy results from plasma volume expansion by a factor of 5–8, the same as for planar geometry. In Sec. VI conclusions are presented.

## II. THE EXPERIMENTAL RESULTS

As a part of a spectroscopic research of the anode plasma at the MID of the Weizmann Institute, we performed a detailed study of the ion velocities. Figure 1 (taken from Ref. 1) shows the blue shift of the CIII 2297 Å

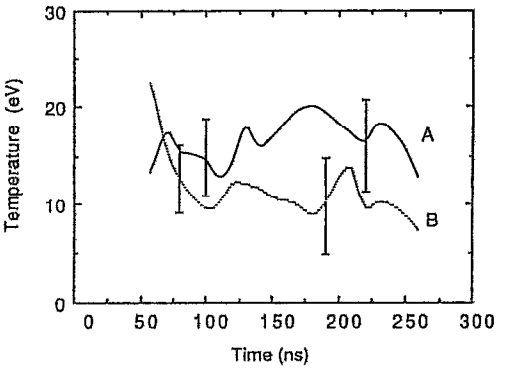


FIG. 2. Position averaged CIII temperatures obtained using the 2297 Å line for the $y$ direction ($A$) and the $z$ direction ($B$).

line measured at 53° with the normal to the anode ($N$) and the shift measured parallel to the anode ($P$). The shift ($N$) corresponds to velocity that decreases from 1 cm/$\mu$sec ($\simeq$15 eV) at time 50 nsec to 0.5 cm/$\mu$sec at 100 nsec, while the shift $P$ corresponds to velocities less than 0.1 cm/$\mu$sec. This measurement shows clearly that the ions have a flow velocity in a direction perpendicular to the anode. Figure 2 shows the position averaged CIII temperatures obtained using the same line as in Fig. 1 for the $z$ direction ($B$) (parallel to the magnetic field) and for the $y$ direction ($A$) (normal to the magnetic field and parallel to the anode surface). Both temperatures are approximately the same (10–20 eV). This thermal energy is similar to the kinetic energy associated with the directed motion normal to the anode surface that is shown in Fig. 1.

In addition to the analysis of line shapes of spontaneous emission, we employed techniques of laser absorption which enabled us to measure ion temperatures as close as 30 $\mu$m to the anode surface. Figure 3 (taken from Ref. 3) shows the profile of a MgII absorption line obtained within 30 $\mu$m from the anode and the profile of a MgII spontaneous emission line obtained within 100 $\mu$m to the anode

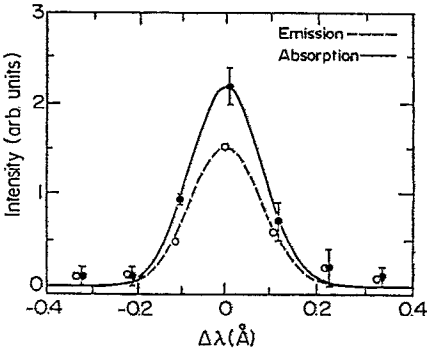


FIG. 3. Absorption and emission Doppler broadened profiles for an MgII transition. The wavelength $\Delta\lambda$ is with respect to the line center. The profiles of the absorption line ($3S_{1/2} \rightarrow 3P_{1/2}$) and that of the spontaneous emission ($3P_{3/2} \rightarrow 3S_{1/2}$) are obtained within $\simeq$30 $\mu$m and $\simeq$100 $\mu$m, respectively, from the anode surface. The two profiles were measured simultaneously for $t = 55$ nsec. The uncertainty in each data point for the emission profile is $\pm 15\%$ (not shown in the figure).



Downloaded 04 Feb 2004 to 132.77.4.129. Redistribution subject to AIP license or copyright, see http://pop.aip.org/pop/copyright.jsp

surface. Both profiles show a similar temperature of $\simeq 15$ eV. This was the same temperature that we observed at larger distances from the anode surface.

The measurements described above show an ion flow velocity of 10–20 eV in a direction perpendicular to the anode surface. The ions have a temperature parallel to the anode surface (both parallel and perpendicular to the magnetic field) of 10–20 eV as well. This velocity and temperature seem to be acquired by the ions very close to the anode surface, within 30 $\mu$m. Our goal in the present paper is to suggest mechanisms that could generate such ion flow velocity and temperature at such a short distance from the anode.

## III. THE MODEL

We assume that a plasma is generated in a small region, few tens of micrometers wide, near the anode. The density there is larger than the density of the background plasma (which is $\lesssim 2\times 10^{15}$ cm$^{-3}$). The plasma within the region of the increased density flows into the background plasma. This motion is characterized as follows: (1) the time of flight (few nsec) is much shorter than the ion cyclotron period which is, for the 7 kG magnetic field, equal or larger than 100 nsec and much shorter than the ion collision time (which is larger than 10 nsec). The ions are therefore collisionless and unmagnetized. Also, the ion kinetic energy is associated only with its directed velocity. We therefore describe the ion dynamics by the momentum equation of a cold fluid

$$M\left(\frac{\partial}{\partial t}+\mathbf{v}\cdot\nabla\right)\mathbf{v}=-e\nabla\phi. \tag{1}$$

Here $e$ and $M$ are the ion charge and mass, $\mathbf{v}$ is the ion velocity, and $\phi$ is the electrostatic potential. (2) The electrons are assumed to be in thermal equilibrium so that we can neglect their inertia. This is equivalent to the assumption that the electron thermal velocity is much larger than its directed velocity. Therefore

$$0=-e\left(-\nabla\phi+\frac{\mathbf{v}_e\times B_0\hat{e}_z}{c}\right)-\frac{\nabla P_e}{en_e}-m\nu_{eN}\mathbf{v}_e -m\nu_{ei}(\mathbf{v}_e-\mathbf{v}). \tag{2}$$

Here $n_e$, $\mathbf{v}_e$, $P_e$, and $m$ are the electron density, directed velocity, pressure, and mass. The electrons are assumed collisional or magnetized enough so that their pressure is isotropic. We also allow electron collisions with stationary neutrals of frequency $\nu_{eN}$ and collisions with ions of frequency $\nu_{ei}$. We assume further that all quantities depend on $x$ only. We add Eqs. (1) and (2), and obtain

$$\left(\frac{\partial}{\partial t}+v_x\frac{\partial}{\partial x}\right)v_x=-\frac{1}{\rho}\frac{\partial P_e}{\partial x}-\frac{m}{M}\nu_e, \tag{3}$$

where

$$\nu_e\equiv\nu_{eN}+\omega_c^2/(\nu_{eN}+\nu_{ei}), \tag{4}$$

also $\rho\equiv Mn$ and $\omega_c\equiv eB_0/mc$. The second term on the right-hand side of (3) is small relative to the first term provided

$$\frac{v_{\rm th}}{v_{ex}}\gg\frac{L}{v_{\rm th}}\nu_e. \tag{5}$$

Here $L$ is the width of the layer and $v_{\rm th}$ is the electron thermal velocity. If the electrons are magnetized $\omega_c\gg\nu_{eN},\nu_{ei}$, the collision frequency is $\nu_e=\omega_c^2/(\nu_{eN}+\nu_{ei})$ and inequality (5) becomes

$$\frac{r_L^2}{L}\frac{(\nu_{eN}+\nu_{ei})}{v_e}\gg 1. \tag{6}$$

In the anode plasma the electron collision frequency was found to be one-fourth of the electron cyclotron frequency, and about ten times larger than Spitzer's collision frequency.[1,15] In the plasma near the anode $r_L\gtrsim 7$ $\mu$m, $L\leqslant 50$ $\mu$m, $(\nu_{eN}+\nu_{ei})\gtrsim\omega_c/4=2\times 10^{10}$ sec$^{-1}$, and $v_e$ is a few cm/$\mu$sec. The left-hand side of (6) is larger than 1, and, therefore, inequality (5) seems to be satisfied to a good approximation even for the magnetized case. If $\nu_{ei}$ is larger than $\nu_{eN}$ and $\omega_c$, $\nu_e$ is even smaller and inequality (5) is clearly satisfied. In most of this paper we therefore neglect the last term in Eq. (3). We will, however, also address the case that collisions with neutrals are dominant and $\nu_e\cong\nu_N$ which is large enough so that (5) is not valid. For such a case $\nu_N$ has to be larger than $10^{11}$ sec$^{-1}$ and the neutral density larger than $2\times 10^{18}$ cm$^{-3}$. We require, however, that either $v_{\rm th}/\nu$ or $r_L$ be smaller than $L$, so that we can still assume that the electron pressure is isotropic.

The electron pressure is assumed to satisfy a polytropic equation of state

$$P_e=A\rho^\gamma, \tag{7}$$

where $\gamma$ is the ratio of specific heats. Since the plasma density is high we require quasineutrality $n_e\cong n$. For our $\sim 10$ eV electron temperature plasma of $n_e\lesssim 2\times 10^{15}$ cm$^{-3}$, the Debye length is smaller than 0.5 $\mu$m. We therefore require that $L\gg 0.5$ $\mu$m.

We complement Eqs. (3) and (7) by the continuity equation

$$\frac{\partial\rho}{\partial t}+\nabla\cdot\rho\mathbf{v}=s(\mathbf{r}), \tag{8}$$

where $s$ is a source and sink function of ionization, recombination, and so on.

For both slab and spherical geometries, we will now find the plasma evolution for the following cases:

(1) The plasma is constantly supplied with ionizations. We calculate the steady state $s(\mathbf{r})\neq 0$, $\partial/\partial t=0$.

(2) The plasma is generated in a time much shorter than the expansion time. We solve for the time dependence of the plasma where $s(\mathbf{r})=0$, $\partial/\partial t\neq 0$.

## IV. SOLUTIONS IN SLAB GEOMETRY

We assume that a high-density layer of neutrals exists near the anode. The plasma is therefore produced in a localized area near the anode. In our model we take the



Downloaded 04 Feb 2004 to 132.77.4.129. Redistribution subject to AIP license or copyright, see http://pop.aip.org/pop/copyright.jsp

neutral cloud to be symmetric about $x=0$, (the anode surface). A plasma density hump, accompanied by a potential hump, therefore forms, symmetric about $x=0$. The ions are accelerated as they slide down the potential hill, while the electrons lose some of their thermal energy. The real neutral cloud corresponds to the half-cloud which occupies $x>0$. We therefore consider the flow of ions which are generated in this half of the cloud, all of which flow away from the $x=0$ surface. We look for the time-independent profiles of density, electric potential, electron temperature, and ion velocity.

All the quantities depend on $x$ only, the distance from the wall. The ions are assumed collisionless. The ion density is

$$n_i(x)=\int_0^x \frac{dx'\, g(x')}{w(x,x')}. \tag{9}$$

Here $g(x')$ is the rate of ion generation and $w(x,x')$ is the velocity at $x$ of an ion which was born at $x'$

$$e\phi(x)+\frac{Mw^2}{2}=e\phi(x'). \tag{10}$$

The ion generation rate is

$$g(x)=\chi n_e(x) n_N(x). \tag{11}$$

Here, $n_e(x)$ and $n_N(x)$ are the electron and neutral densities and $\chi\equiv\sigma_e v_e$, where $\sigma_e$ is the cross section for ionization by electrons. We assume that

$$n_N(x)=N_0 e^{-x/\lambda}. \tag{12}$$

The electrons satisfy Eq. (2) and have a polytropic equation of state (7). We assume that inequality (5) holds, and thus

$$n_e(x)=n_0\left[1+\left(\frac{\gamma-1}{\gamma}\right)\frac{e\phi}{T_0}\right]^{1/(\gamma-1)}, \tag{13}$$

where $n_0$ and $T_0$ are the electron density and temperature at $x=0$, where $\phi(x=0)=0$. In writing Eq. (13) we assume that $\gamma>1$, and exclude the isothermal case ($\gamma=1$). We restrict ourselves to the quasineutral case, and thus

$$\frac{1}{\alpha}\left[1+\left(\frac{\gamma-1}{\gamma}\right)\Psi\right]^{1/(\gamma-1)} = \int_0^\xi \frac{d\xi'\, e^{-\xi'}\{1+[(\gamma-1)/\gamma]\Psi'\}^{1/(\gamma-1)}}{(\Psi'-\Psi)^{1/2}}, \tag{14}$$

where $\Psi\equiv e\phi/T_0$, $\xi\equiv x/\lambda$, and $\Psi'\equiv\Psi(\xi')$. Also, we define here $\alpha\equiv\nu_i/\nu_{\rm tr}$, where $\nu_i\equiv\chi N_0$ is the ionization frequency at $x=0$, and $\nu_{\rm tr}\equiv(2T_0/M_i)^{1/2}/\lambda$ is a typical inverse transit time for an ion moving across the neutral layer. This is a version of the well-known plasma equation[16–19] in the quasineutral approximation.

Before finding solutions to Eq. (14), we consider whether energy is conserved by the system it describes. Ions have initially zero kinetic energy, so the normalized ion energy flux at $\xi$ is

$$\Gamma_i^E=\int_0^\xi d\xi'\, e^{-\xi'}\left(1+\frac{\gamma-1}{\gamma}\Psi(\xi')\right)^{1/(\gamma-1)} \times[\Psi(\xi')-\Psi(\xi)]. \tag{15}$$

It can be shown that the electron equation of state [Eq. (7)] implies that electrons generated by ionization have an initial average kinetic energy of $[\gamma/(\gamma-1)]T$. Therefore, the electron energy flux is

$$\Gamma_e^E=\int_0^\xi d\xi'\, e^{-\xi'}\left(1+\frac{\gamma-1}{\gamma}\Psi(\xi')\right)^{1/(\gamma-1)} \times\frac{\gamma}{\gamma-1}\left(1+\frac{\gamma-1}{\gamma}\Psi(\xi)\right). \tag{16}$$

(That the initial electron energy $\{[\gamma/(\gamma-1)]T\}$ is larger than the thermal energy $\{[1/(\gamma-1)]T\}$, is not surprising. The reason that ion heating occurs is that these more energetic electrons give up some of their energy to the ions before becoming thermalized.) We now compare these fluxes to the energy generation rate ($S^E$) between 0 and $\xi$:

$$S^E=\int_0^\xi d\xi'\, e^{-\xi'}\left(1+\frac{\gamma-1}{\gamma}\Psi(\xi')\right)^{1/(\gamma-1)} \times\frac{\gamma}{\gamma-1}\left(1+\frac{\gamma-1}{\gamma}\Psi(\xi')\right). \tag{17}$$

The expression $(\Gamma_i^E+\Gamma_e^E)-S^E$ is identically zero, as is necessary for energy conservation.

As is well known, Eq. (14) can be solved for $\xi(\Psi)$. We multiply both sides of the equation by $(\Psi-\Psi_1)^{-1/2}$ and integrate on $\Psi$ from zero to $\Psi_1$, after we make $\Psi$ rather than $\xi$ the independent variable in the integral on the right-hand side. The result of the integration is

$$\frac{1}{\alpha}G(\Psi)=\pi\int_0^\Psi d\Psi'\frac{d\xi'}{d\Psi'}e^{-\xi'}\left[1+\left(\frac{\gamma-1}{\gamma}\right)\Psi'\right]^{1/(\gamma-1)} \tag{18}$$

where we wrote $\Psi$ instead of $\Psi_1$, and

$$G(\Psi)\equiv\int_0^\Psi\frac{d\Psi'}{(\Psi'-\Psi)^{1/2}}\left[1+\left(\frac{\gamma-1}{\gamma}\right)\Psi'\right]^{1/(\gamma-1)}. \tag{19}$$

Let us choose $\gamma=5/3$. Then

$$G(\Psi)=-\tfrac{5}{4}(1+\tfrac{6}{25}\Psi)(-\Psi)^{1/2}-\tfrac{3}{4}(\tfrac{5}{2})^{1/2}(1+\tfrac{2}{5}\Psi)^2 \times[\ln|1+(-\tfrac{2}{5}\Psi)^{1/2}|-\ln|(1+\tfrac{2}{5}\Psi)^{1/2}|]. \tag{20}$$

In order to simplify the analysis let us approximate the electron density in the expression for $g(x)$ [Eq. (11)] as a constant

$$n_e(x)\cong n_0. \tag{21}$$

The electron density changes less than the neutral density and thus this seems a reasonable approximation. With this approximation Eq. (18) is simplified to



Downloaded 04 Feb 2004 to 132.77.4.129. Redistribution subject to AIP license or copyright, see http://pop.aip.org/pop/copyright.jsp

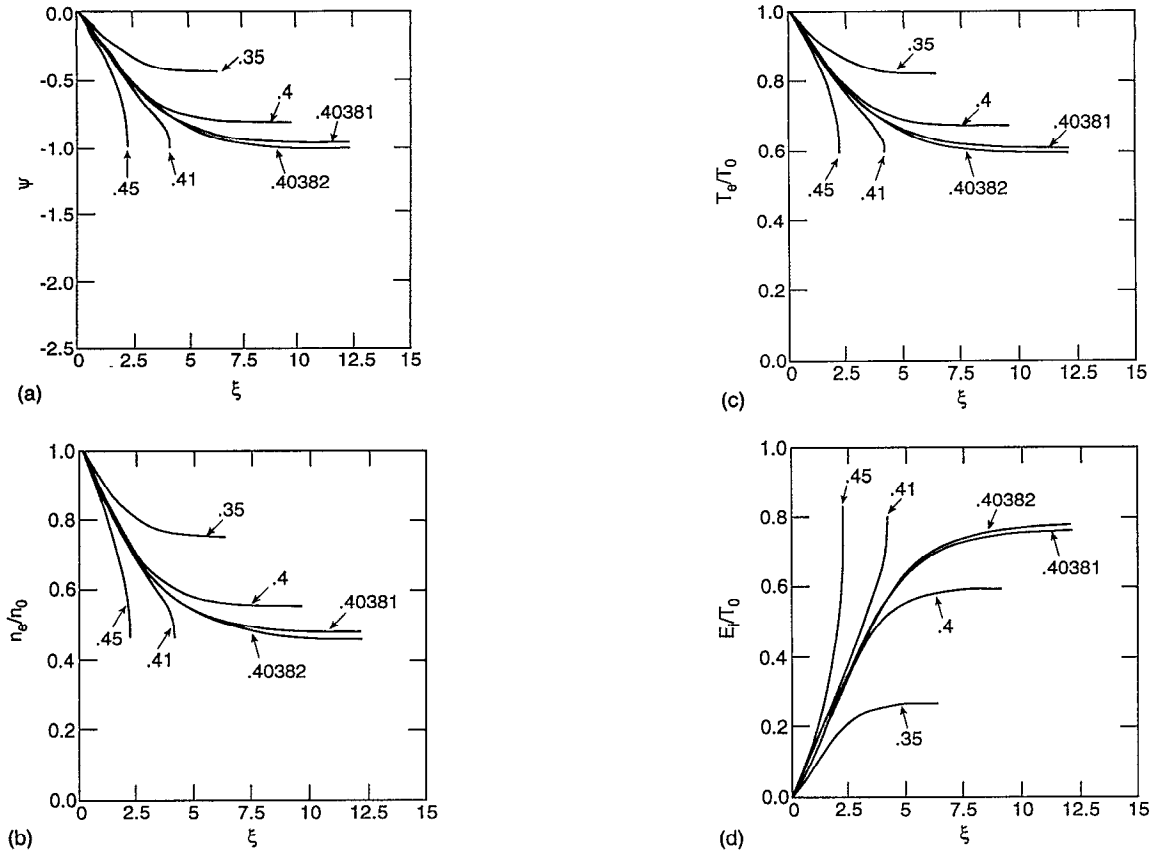


FIG. 4. (a) $\Psi$ vs $\xi$, (b) the normalized density $n_e/n_0$ vs $\xi$, (c) the normalized temperature $T_e/T_0$ vs $\xi$, and (d) the normalized ion energy $E_i/T_0$ vs $\xi$, for various values of $\alpha$.

$$\frac{1}{\alpha}G(\Psi)=\pi(e^{-\xi}-1) \quad \xi\geqslant 0. \tag{22}$$

From Eq. (22), Fig. 4 presents the potential $\Psi$, the normalized electron density (divided by the maximal density), the normalized electron temperature (divided by the maximal temperature), and the normalized ion energy as functions of $\xi$. The plots are given for several values of the parameter $\alpha$. For $\alpha<\alpha^*=0.404$, the potential $\Psi$ is continuous for $\xi\to\infty$. Here ion heating occurs in a steady-state manner, with up to $0.77T_0$ of the electron energy being transferred to ions.

For $\alpha>\alpha^*$, $\Psi$ becomes singular for finite $\xi$, and the assumption of quasineutrality breaks down. We have solved the full Poisson equation for this case, and have found that this breakdown of quasineutrality corresponds to the disappearance of steady-state flow. Physically, this can be understood as follows: Increasing $\alpha$ corresponds to increasing the ionization rate $\nu_i$. For a steady-state solution, more rapid ionization necessitates larger ion flow, therefore a larger drop in potential $\Psi$. As $\Psi$ decreases, however, the electron density also decreases, thus restricting the ion flow. Therefore, increasing the drop in potential $\Psi$ becomes less and less effective at increasing the ion flow. Thus we find the critical value $\alpha=\alpha^*$, above which the ion flow cannot match the ion generation rate, regardless of the size of the potential drop in $\Psi$. For $\alpha>\alpha^*$, therefore, a steady-state flow is not possible. In reality the neutral density (12) is not specified but affected by the process of ionization itself. The neutral layer dimension will be adjusted so that $\alpha<\alpha^*$.

We now solve for the time-dependent expansion in slab geometry. We assume the plasma is generated on a time much smaller than $L/v$ where $L$ and $v$ are characteristic length and velocity scales. The flow of neutrals ceases and the plasma then expands until its density equals the density of the background plasma. The reduction in temperature is $T_f/T_i=(\rho_f/\rho_i)^{\gamma-1}=(L_f/L_i)^{-d(\gamma-1)}$. Here $i,f$ denote initial and final, $L$ is a characteristic dimension, and $d=1$, 2, or 3 is the dimensionality parameter. The isotropic velocity distribution we measured suggests that $\gamma=5/3$. If the expansion is one dimensional $d=1$,

$$\left(\frac{T_f}{T_i}\right)_{1D}=\left(\frac{L_f}{L_i}\right)^{-2/3}. \tag{23}$$

If the electron temperature decreases to a fourth and the rest of the energy becomes ion directed energy we obtain final ion energy three times the electron energy. It is therefore required that the plasma dimension increase by a factor $\sim 8$ for such an energy transfer.

This estimate is consistent with the following explicit self-similar solution. For a time-dependent expansion, we take $s(r)$ to be zero in Eq. (8). The governing equations become



Downloaded 04 Feb 2004 to 132.77.4.129. Redistribution subject to AIP license or copyright, see http://pop.aip.org/pop/copyright.jsp

$$\left(\frac{\partial}{\partial t}+v\frac{\partial}{\partial x}\right)v=-\frac{A\gamma}{(\gamma-1)}\frac{\partial}{\partial x}\rho^{\gamma-1}-\nu v \tag{24}$$

and

$$\frac{\partial\rho}{\partial t}+\frac{\partial}{\partial x}(\rho v)=0, \tag{25}$$

where $v$ is the fluid velocity. These two equations represent the expansion of a polytropic gas. In our case the expansion is into the background plasma, but for simplicity we examine expansion into vacuum. We will look for a solution which is symmetric about the anode surface ($x=0$). We then consider the ion flow and heating for $x>0$. For the initial density

$$\rho(x,t=0)=\rho_{c0}\left(1-\frac{x^2}{X_0^2}\right)^{1/(\gamma-1)}, \tag{26}$$

there is a self-similar solution of Eqs. (24) and (25). A solution for the analogous problem in spherical geometry, without the drag force, was given in Ref. 20. For convenience we write the equations in nondimensional units. The initial electron temperature at the center is $P_{c0}/n_{c0}=A\rho_{c0}^{\gamma}M/\rho_{c0}=T_{c0}$, $A=T_{c0}\rho_{c0}^{1-\gamma}/M$. We normalize $x$ by $X_0$, $\rho$ by $\rho_{c0}$, $v$ by $v_s=(T_0/M)^{1/2}$, $t$ by $X_0/v_s$, and $\nu$ by $v_s/X_0$. Equations (24)–(26) become

$$\left(\frac{\partial}{\partial t}+v\frac{\partial}{\partial x}\right)v=-\frac{\gamma}{(\gamma-1)}\frac{\partial}{\partial x}\rho^{\gamma-1}-\nu v,$$

$$\frac{\partial\rho}{\partial t}+\frac{\partial}{\partial x}(\rho v)=0, \tag{27}$$

$$\rho(x,t=0)=(1-x^2)^{1/(\gamma-1)}, \tag{28}$$

for $x\leqslant 1$. The solution of these equations, similarly to Ref. 20, is

$$\rho(x,t)=\rho_c(t)\left(1-\frac{x^2}{X(t)^2}\right)^{1/(\gamma-1)}. \tag{29}$$

Also

$$\rho_c(t)X(t)=1, \tag{30}$$

where

$$\rho_c(0)=X(0)=1. \tag{31}$$

The velocity is

$$v(r,t)=\dot{X}(t)x/X(t) \tag{32}$$

for $x\leqslant X(t)$. The equation of motion for the radius $X$ is

$$\ddot{X}=\frac{2\gamma}{(\gamma-1)X^{\gamma}}-\nu\dot{X}. \tag{33}$$

In the first phase of the expansion, the drag term is small and the plasma is accelerated. When the two terms on the right-hand side of the equation become comparable, the plasma velocity reaches its maximum and starts to decrease. At these later times $\ddot{X}$ is small and

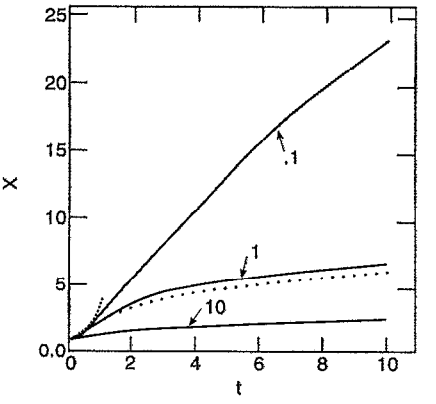


FIG. 5. $X$ vs $t$, for $\nu=0.1$, 1, 10. The dotted curves show the approximate results [(36) and (37)] for $\nu=1$.

$$X\cong\left(\frac{2\gamma(\gamma+1)}{\nu(\gamma-1)}t\right)^{1/(\gamma+1)}. \tag{34}$$

The velocity $\dot{X}$ approaches zero asymptotically. At earlier times we neglect collisions and the solution of (33) without the second term on the right-hand side is

$$t=\frac{\gamma-1}{2\gamma^{1/2}}\int_1^X\frac{dx}{(1-x^{1-\gamma})^{1/2}}. \tag{35}$$

Figure 5 shows $X$ as a function of $t$ for various values of $\nu$ for $\gamma=5/3$. For $\nu=1$, which corresponds to a neutral density of $10^{18}$ cm$^{-3}$, we plot also the approximate relations (34) and (35) which become

$$X=\left(\frac{40}{3\nu}t\right)^{3/8}, \quad t\to\infty \tag{36}$$

and

$$X=1+\tfrac{5}{2}t^2, \quad t\to 0. \tag{37}$$

It seems that unless the neutral density is very large ($10^{18}$ cm$^{-3}$) we can neglect the collision term ($\nu\dot{X}$) in (33). We therefore examine the rate of energy transfer from electrons to ions when collisions are neglected. The electron thermal energy $E_T=\frac{3}{2}\int_0^X dx\,P_e(x,t)$ and the ion directed energy $E_k=\int_0^X dx\,\frac{1}{2}\rho v(x,t)^2$ are

$$E_T(t)=\frac{3}{2}\frac{1}{X(t)^{2/3}}\int_0^1 dx(1-x^2)^{5/2} \tag{38}$$

and

$$E_k(t)=\frac{3}{2}\left(1-\frac{1}{X^{2/3}}\right)\int_0^1 dx(1-x^2)^{5/2}, \tag{39}$$

where we used the relation $(\dot{X})^2=15(1-1/X^{2/3})$. We obtain

$$E_k/E_T=X^{2/3}-1. \tag{40}$$

For ion energy two to three times the electron energy $X$ has to be a factor of 5–8. This is consistent with the conclusions drawn from Eq. (23). Assume that at this value the average density in the slab is equal to the density of the plasma



Downloaded 04 Feb 2004 to 132.77.4.129. Redistribution subject to AIP license or copyright, see http://pop.aip.org/pop/copyright.jsp

background. The average density of the slab is then initially five to eight times the background density.

For both steady-state and time-dependent expansions we find ion heating in the range observed in experiments. Thus, the slab model we presented can explain the higher ion energies. It does not, however, explain the almost isotropic ion distribution. In the next section we solve the steady-state and time-dependent cases in spherical geometry in order to account for that isotropy.

## V. SOLUTIONS IN SPHERICAL GEOMETRY

We consider now the case of steady-state flow in spherical geometry. We assume that a ball of neutrals has a density

$$n_N(r)=N_0 e^{-r^2/\lambda^2}, \tag{41}$$

where $r$ is the radial position in spherical coordinates. The center of the ball is at $x=0$, the anode surface. We are therefore actually interested in the ion flow from a half-ball on the anode surface, but for simplicity we consider the spherically symmetric case. The electron density satisfies Eq. (13) with $\gamma=5/3$,

$$n_e=n_0(1+\tfrac{2}{5}\Psi)^{3/2}. \tag{42}$$

In spherical symmetry we obtain the equation

$$\frac{1}{\alpha}\left(1+\frac{2}{5}\Psi\right)^{3/2}=\int_0^\rho \frac{d\rho'\ \rho'^2(1+\frac{2}{5}\Psi')^{3/2}e^{-\rho'^2}}{\rho^2(\Psi'-\Psi)^{1/2}}, \tag{43}$$

where $\rho\equiv r/\lambda$.

Energy conservation for Eq. (43) is shown similarly to that for the steady-state slab in Sec. IV. The ion energy flux at $\rho$ is

$$\Gamma_i^E=\int_0^\rho d\rho'\ \rho'^2 e^{-\rho'^2}\left(1+\frac{\gamma-1}{\gamma}\Psi(\rho')\right)^{1/(\gamma-1)} \times[\Psi(\rho')-\Psi(\rho)]. \tag{44}$$

The electron energy flux at $\rho$ is

$$\Gamma_e^E=\int_0^\rho d\rho'\rho'^2 e^{-\rho'^2}\left(1+\frac{\gamma-1}{\gamma}\Psi(\rho')\right)^{1/(\gamma-1)} \times\frac{\gamma}{\gamma-1}\left(1+\frac{\gamma-1}{\gamma}\Psi(\rho)\right). \tag{45}$$

The energy generation rate within radius $\rho$ is

$$S^E=\int_0^\rho d\rho'\ \rho'^2 e^{-\rho'^2}\left(1+\frac{\gamma-1}{\gamma}\Psi(\rho')\right)^{1/(\gamma-1)} \times\frac{\gamma}{\gamma-1}\left(1+\frac{\gamma-1}{\gamma}\Psi(\rho')\right). \tag{46}$$

The expression $(\Gamma_i^E+\Gamma_e^E)-S^E$ is identically zero, as is necessary for energy conservation.

In Fig. 6(a) we plot $\Psi$ vs $\rho$, from the numerical solution of Eq. (43), for several values of $\alpha$. Figures 6(b) and 6(c) show the electron and ion energies. Steady-state ion heating (and electron cooling) is largest for $\alpha\simeq 1.76$. In this case, about two-thirds of the electron energy is converted to ion energy. The ion heating rapidly decreases with decreasing $\alpha$. For $\alpha>1.76$, the solution for $\Psi$ becomes singular, indicating the absence of a steady-state flow.

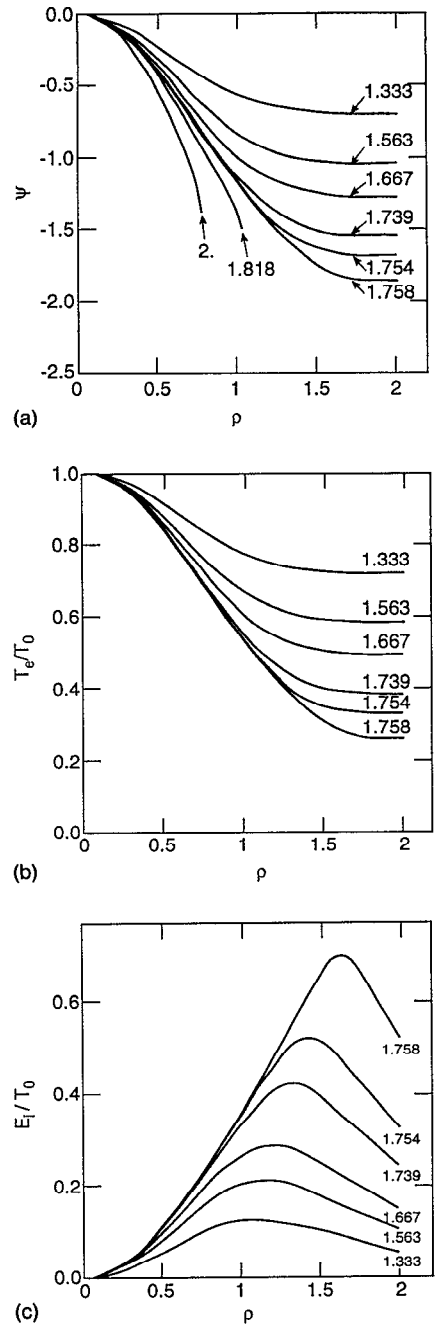


FIG. 6. (a) $\Psi$ vs $\rho$, (b) the normalized temperature $T_e/T_0$ vs $\rho$, and (c) the normalized ion energy $E_i/T_0$ vs $\rho$, for various values of $\alpha$.

We now consider time-dependent expansion in spherical geometry. This corresponds to $\alpha>1.76$ for the neutral ball described by Eq. (41). Let us examine the idealized problem of the expansion of a plasma ball. As with the steady-state expansion, the presence of the anode does not allow spherical symmetry in our case. However, for simplicity we treat a half-ball as a full ball. The reduction of temperature is $T_f/T_i=(L_f/L_i)^{-d(\gamma-1)}=(L_f/L_i)^{-2}$. If



Downloaded 04 Feb 2004 to 132.77.4.129. Redistribution subject to AIP license or copyright, see http://pop.aip.org/pop/copyright.jsp

the electron temperature decreases to one-fourth and the rest of the energy becomes ion directed energy we obtain final ion energy three times the electron energy. It is therefore sufficient that the plasma dimension doubles itself for such an energy transfer.

We demonstrate the above estimate again with a self-similar solution. As in Sec. IV, we take $s(r)$ to be zero for the time-dependent expansion. The governing equations become

$$\left(\frac{\partial}{\partial t}+v\frac{\partial}{\partial r}\right)v=-\frac{A\gamma}{(\gamma-1)}\frac{\partial}{\partial r}\rho^{\gamma-1}-\nu v \tag{47}$$

and

$$\frac{\partial\rho}{\partial t}+\frac{1}{r^2}\frac{\partial}{\partial r}(r^2\rho v)=0, \tag{48}$$

where $v$ is the radial component of the velocity. The self-similar solution to this system is almost identical to that in slab geometry (Sec. IV), and is given in Ref. 21 for $\nu=0$. We obtain

$$\rho(r,t)=\rho_c(t)\left(1-\frac{r^2}{R(t)^2}\right)^{1/(\gamma-1)}, \tag{49}$$

where

$$\rho_c(t)R(t)^3=1 \tag{50}$$

and

$$\rho_c(0)=R(0)=1. \tag{51}$$

Here, we normalize $r$ by $R_0$, $\rho$ by $\rho_{c0}$, $v$ by $v_s=(T_0/M)^{1/2}$, $t$ by $R_0/v_s$, and $\nu$ by $v_s/R_0$. The velocity is

$$v(r,t)=\dot{R}(t)r/R(t) \tag{52}$$

for $r\leqslant R(t)$. The equation of motion for the radius $R$ is

$$\ddot{R}=\frac{2\gamma}{(\gamma-1)R^{3\gamma-2}}-\nu\dot{R}. \tag{53}$$

At later times $\ddot{R}$ is small and

$$R\cong\left(\frac{2\gamma(3\gamma-1)}{\nu(\gamma-1)}t\right)^{1/(3\gamma-1)}=\left(\frac{20}{\nu}t\right)^{1/4}\quad t\to\infty. \tag{54}$$

The velocity $\dot{R}$ approaches zero asymptotically. At earlier times we neglect collisions and the solution of (53) without the second term on the right-hand side is

$$R=(1+5t^2)^{1/2},\quad t\to 0. \tag{55}$$

Figure 7 shows $R$ as a function of $t$ for various values of $\nu$ for $\gamma=5/3$. For $\nu=1$, which corresponds to a neutral density of $10^{18}$ cm$^{-3}$, we plot also the approximate relations (54) and (55).

Unless the neutral density is very large ($10^{18}$ cm$^{-3}$) we can neglect the collision term in (53). When collisions are neglected, the electron thermal energy $E_T=\frac{3}{2}\int_0^R dr\,4\pi r^2P_e(r,t)$ and the ion directed energy $E_k=\int_0^R dr\,4\pi r^2\frac{1}{2}\rho v(r,t)^2$ are

$$E_T(t)=\frac{6\pi}{R(t)^2}\int_0^1 dx\,x^2(1-x^2)^{5/2} \tag{56}$$

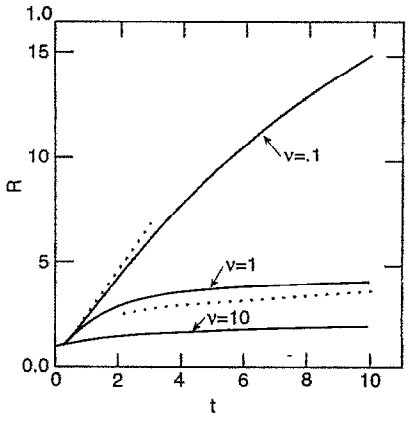


FIG. 7. $R$ vs $t$, for $\nu=0.1$, 1, 10. The dotted curves show the approximate results [(54) and (55)] for $\nu=1$.

and

$$E_k(t)=6\pi\left(1-\frac{1}{R^2}\right)\int_0^1 dx\,x^2(1-x^2)^{5/2}, \tag{57}$$

where we used the relation $(\dot{R})^2=5(1-1/R^2)$. We obtain

$$E_k/E_T=R^2-1. \tag{58}$$

For ion energy two to three times the electron energy $R$ has to be 1.7–2. Assume that at this value the average density in the ball is equal to the density of the plasma background. The average density of the ball is then initially five to eight times the background density.

The time-dependent spherical expansion has the following features: a plasma generated as a ball of density few times $10^{16}$ cm$^{-3}$, one order of magnitude larger than that of the plasma density, and composed initially of cold ions and electrons of temperature $\sim$30 eV expands. By the time the density of the ball becomes equal to the density of the background plasma the electron temperature is about 10 eV and the singly charged ion kinetic energy is about 20 eV. The initial radius is less than 30 $\mu$m and the final radius of the ball is smaller than 50 $\mu$m.

The lower bound on the ball radius is not clear. If the initial ball radius is much smaller than the electron Larmor radius and the collision mean-free path the expansion would be collisionless. There is no clear way to show it is not so. However, the ball radius seems to be related to nonuniformities in the anode and they should determine the initial ball dimensions.

A consequence of the localized plasma generation is the presence of strong electric fields near the anode, of intensity 10 kV/cm. The assumption that plasma is generated and expands in a few nsec results in fluctuations of the electric field with frequency of $10^9$ sec$^{-1}$. Such strong oscillations were in fact measured in all the plasma.[21]

## VI. CONCLUSIONS

We examined several pictures of energetic ion generation in the anode plasma. We assumed that a dense plasma is generated in a small region near the anode and during its



Downloaded 04 Feb 2004 to 132.77.4.129. Redistribution subject to AIP license or copyright, see http://pop.aip.org/pop/copyright.jsp

expansion into the background plasma electrons transfer their thermal energy into ion directed kinetic energy. Both time-dependent and steady-state plasma expansions were examined for a slab and spherical geometries. While the amount of energy transferred from the electrons to ions is not very sensitive to the geometry, a plasma generation in "half-balls" could explain the isotropy of the ion energies, while a slab plasma should result in anisotropic ion velocity distribution. Thus, our model could explain the three main observations related to the ion velocities: the magnitude of the ion flow velocity normal to the anode surface, the isotropy of ion velocity distribution parallel to the anode surface, and the ion acceleration very close to the anode surface. Our model assumes higher electron temperature and density near the anode. We are currently using our spectroscopic methods to measure with high spatial resolution the plasma parameters near the anode.

The source of the ion energy in the picture we suggest is the electron thermal energy. Possible sources for a high electron thermal energy near the anode should be investigated further.

## ACKNOWLEDGMENTS

The authors are grateful to S. Eliezer, R. Boxman, S. Goldsmith, N. Hershkowitz, E. Sarid, and Z. Zinamon for useful discussions, and to L. P. Harris for sending them some of his work.

This work is partially supported by the Feinberg school.

[1] Y. Maron, E. Sarid, O. Zahavi, L. Perelmutter, and M. Sarfaty, Phys. Rev. A **39**, 5842 (1989).
[2] Y. Maron, L. Perelmutter, E. Sarid, M. E. Foord, and M. Sarfaty, Phys. Rev. A **41**, 1074 (1990).
[3] L. Perelmutter, G. Davara, and Y. Maron, Bull. Am. Phys. Soc. **35**, 2120 (1990).
[4] A. A. Plyutto, V. N. Ryzkov, and A. T. Kapin, Sov. Phys. JETP **20**, 328 (1965).
[5] W. D. Davis and H. C. Miller, J. Appl. Phys. **40**, 2212 (1969).
[6] F. M. Bacon and H. A. Watts, J. Appl. Phys. **46**, 4758 (1975).
[7] L. P. Harris, IEEE Trans. Plasma Sci. **PS-11**, 94 (1983).
[8] S. Goldsmith and R. L. Boxman, J. Appl. Phys. **51**, 3649 (1980).
[9] P. M. Campbell, R. R. Johnson, F. J. Mayer, L. V. Powers, and D. C. Slater, Phys. Rev. Lett. **39**, 274 (1977).
[10] R. Decoste and B. M. Ripin, Phys. Rev. Lett. **40**, 34 (1978).
[11] A. V. Gurevich, L. V. Pariiskaya, and L. P. Pitaevskii, Zh. Eksp. Teor. Fiz. **49**, 647 (1965) [Sov. Phys. JETP **22**, 449 (1966)].
[12] J. E. Allen and J. G. Andrews, J. Plasma Phys. **4**, 187 (1970).
[13] K. E. Lonngren and N. Hershkowitz, IEEE Trans. Plasma Sci. **PS-7**, 107 (1979).
[14] S. Eliezer and H. Hora, Phys. Rep. **172**, 341 (1989).
[15] Y. Maron, M. Sarfaty, L. Perelmutter, O. Zahavi, M. E. Foord, and E. Sarid, Phys. Rev. A **40**, 3240 (1989).
[16] L. Tonks and I. Langmuir, Phys. Rev. **34**, 876 (1929).
[17] E. R. Harrison and W. B. Thompson, Proc. Phys. Soc. (London) **74**, 145 (1959).
[18] S. A. Self, Phys. Fluids **6**, 1762 (1963).
[19] K.-U. Riemann, Phys. Fluids **24**, 2163 (1981).
[20] Y. B. Zel'dovich and Y. P. Raizer, in *Physics of Shock Waves and High-Temperature Hydrodynamic Phenomena* (Academic, New York, 1966), p. 104.
[21] E. Sarid, Y. Maron, and L. Troyansky, "Spectroscopic investigation of fluctuating anisotropic electric fields in a high-power-diode plasma," to appear in Phys. Rev. E.



Downloaded 04 Feb 2004 to 132.77.4.129. Redistribution subject to AIP license or copyright, see http://pop.aip.org/pop/copyright.jsp